

Magnetic Anisotropy of a High-Spin Octanuclear Nickel(II) Complex with a *meso*-Helicate CoreEmilio Pardo,[†] Isidoro Morales-Osorio,[†] Miguel Julve,[†] Francesc Lloret,^{*†} Joan Cano,[†] Rafael Ruiz-García,[‡] Jorge Pasán,[§] Catalina Ruiz-Pérez,[§] Xavier Ottenwaelder,^{||} and Yves Journaux^{*||}

Departament de Química Inorgànica, ICMOL, and Departament de Química Orgànica, Universitat de València, 46100 Burjassot, València, Spain, Laboratorio de Rayos X y Materiales Moleculares, Departamento de Física Fundamental II, Universidad de La Laguna, 38204 La Laguna, Tenerife, Spain, and Laboratoire de Chimie Inorganique, Université Paris-XI, 91405 Orsay, France

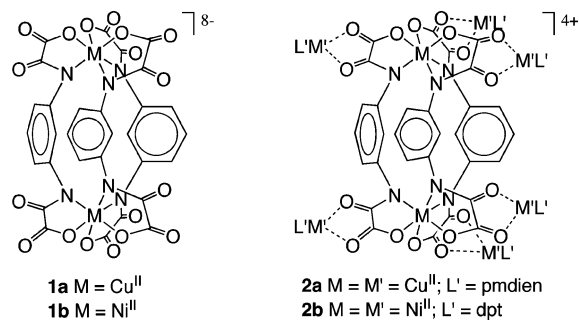
Received July 30, 2004

The octanickel(II) cluster **2b** has been synthesized from the novel ferromagnetically coupled dinickel(II) metallacryptand **1b** assembled from the *m*-phenylene-bis(oxamate) ligand. Complex **2b** exhibits a dimer-of-tetramers structure, with two oxamate-bridged propeller-shaped tetranuclear units connected through three *meta*-substituted phenylenediamidate bridges, giving a metallacryptand core of the *meso*-helicate type. Complex **2b** behaves as a ferromagnetically coupled dimer of two $S = 2$ Ni^{II}_4 units with appreciable magnetic anisotropy.

High-nuclearity coordination clusters of paramagnetic first-row transition metal ions are actively investigated in the field of molecular magnetism for the attainment of single-molecule magnets (SMMs), molecules that exhibit slow relaxation of the magnetization below a blocking temperature (T_B).^{1,2} The design of an SMM targets the attainment of a ground state with both high spin (S) and large negative axial magnetic anisotropy (D), properties that ultimately depend on the nuclearity and topology of the cluster, as well as on the nature of the interacting metal centers and the bridging ligands.^{3,4} Molecular-programmed self-assembly methods, whereby either a multitopic ligand⁵ or a complex⁶ coordinates a metal ion with a preferred coordination geometry, emerge as rational synthetic strategies toward the preparation of SMMs.

We have recently demonstrated that a variety of high-nuclearity copper(II) coordination clusters can be rationally designed and synthesized in this way from self-assembled,

Chart 1



exchange-coupled metallacyclic complexes with aromatic oligooxamate ligands.⁷ In particular, the binuclear copper(II) complex **1a** resulting from the self-assembly of two Cu^{II} ions and three binucleating bridging *N,N'*-1,3-phenylenebis(oxamate) (mpba) ligands (Chart 1, left) is a metallacryptand that can be advantageously used as building block. Through the cis carbonyl oxygen atoms of its oxamate groups, complex **1a** acts as a hexakis(bidentate) ligand toward six other Cu^{II} ions with coordination sites partially blocked by tridentate terminal *N,N,N',N'',N'''*-pentamethyldiethylenetriamine (pmdien) ligands, yielding the octanuclear copper(II) complex **2a** (Chart 1, right).^{7b} When applied with Ni^{II} ions in place of Cu^{II} ions, this step-by-step strategy (the so-called “complex-as-ligand” approach) yields the related dinickel(II) metallacryptand $Na_8[Ni_2(mpba)_3] \cdot 10H_2O$, **1b**, and the

* To whom correspondence should be addressed. E-mail: francisco.lloret@uv.es (F.L.), jour@icmo.u-psud.fr (Y.J.).

[†] Departament de Química Inorgànica, Universitat de València.

[‡] Departament de Química Orgànica, Universitat de València.

[§] Universidad de La Laguna.

^{||} Université Paris-XI.

- (1) Winpenny, R. E. P. *Adv. Inorg. Chem.* **2001**, *52*, 1.
- (2) Gatteschi, D.; Sessoli, R. *Angew. Chem., Int. Ed.* **2003**, *42*, 268.
- (3) Marvaud, V.; Herrera, J. M.; Barilero, T.; Tuyras, F.; Garde, R.; Scullier, A.; Decroix, C.; Cantuel, M.; Desplanches, C. *Monatsh. Chem.* **2003**, *134*, 149.
- (4) Gatteschi, D.; Sorace, L. *J. Solid State Chem.* **2001**, *159*, 253.

- (5) (a) Saalfrank, R. W.; Trummer, S.; Reimann, U.; Chowdhry, M. M.; Hampel, F.; Waldmann, O. *Angew. Chem., Int. Ed.* **2000**, *39*, 3492. (b) Waldmann, O.; Zhao, L.; Thompson, L. K. *Phys. Rev. Lett.* **2002**, *88*, 066401.
- (6) (a) Marvaud, V.; Decroix, C.; Scullier, A.; Guyard-Duhayon, C.; Vaissermann, J.; Gonnet, F.; Verdagner, M. *Chem. Eur. J.* **2003**, *9*, 1677. (b) Choi, H. J.; Sokol, J. J.; Long, J. R. *Inorg. Chem.* **2004**, *43*, 1606.
- (7) (a) Pardo, E.; Bernot, K.; Julve, M.; Lloret, F.; Cano, J.; Ruiz-García, R.; Delgado, F. S.; Ruiz-Pérez, C.; Ottenwaelder, X.; Journaux, Y. *Inorg. Chem.* **2004**, *43*, 2768. (b) Pardo, E.; Bernot, K.; Julve, M.; Lloret, F.; Cano, J.; Ruiz-García, R.; Pasán, J.; Ruiz-Pérez, C.; Ottenwaelder, X.; Journaux, Y. *Chem. Commun.* **2004**, 920. (c) Ottenwaelder, X.; Cano, J.; Journaux, Y.; Riviere, E.; Brennan, C.; Nierlich, M.; Ruiz-García, R. *Angew. Chem., Int. Ed.* **2004**, *43*, 850.

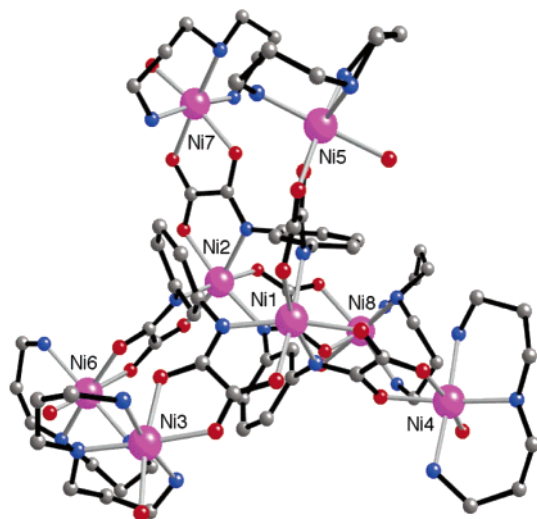


Figure 1. Perspective view of the asymmetric cationic octanickel unit of **2b** with the numbering scheme of the metal atoms.

corresponding octanickel(II) complex $\{[\text{Ni}_2(\text{mpba})_3][\text{Ni}(\text{dpt})(\text{H}_2\text{O})_6]\}(\text{ClO}_4)_4 \cdot 12.5\text{H}_2\text{O}$, **2b**, reported here, with dipropylene-triamine (dpt) as a tridentate terminal ligand (Chart 1).

Precursor **1b** was synthesized from H_4mpba and $\text{Ni}(\text{NO}_3)_2$ in a 3:2 stoichiometry in basic (NaOH) aqueous medium. Complex **2b** was then obtained by reaction of **1b** with the coordinatively unsaturated complex $[\text{Ni}(\text{dpt})]^{2+}$ prepared in situ from a 1:1 mixture of $\text{Ni}(\text{ClO}_4)_2$ and dpt. The crystal structure of **2b** consists of octanuclear nickel(II) cations, $\{[\text{Ni}_2(\text{mpba})_3][\text{Ni}(\text{dpt})(\text{H}_2\text{O})_6]\}^{4+}$ (Figure 1), that are well-separated from each other by perchlorate anions and crystallization water molecules.⁸

The octanickel cation exhibits a dimer-of-tetramers molecular structure. Two oxamate-bridged propeller-like tetranickel units are linked by three *m*-phenylene moieties arranged edge-to-face through weak $\text{C}-\text{H} \cdots \pi$ interactions (average dihedral angle of 60.0° and average centroid-centroid distance of 4.65 \AA). The two central nickel atoms (Ni1 and Ni2) are in a trigonally distorted octahedral NiN_3O_3 geometry [trigonal twist angles of $58.8(6)^\circ$ and $59.0(6)^\circ$] with comparable $\text{Ni}-\text{N}(\text{amidate})$ and $\text{Ni}-\text{O}(\text{carboxylate})$ average bond lengths (2.08 and 2.10 \AA , respectively). These metal sites have opposite Δ and Λ chiralities and are tilted from each other by only $4.7(5)^\circ$ around the Ni1–Ni2 vector. The binuclear metallacryptand core, $[\text{Ni}_2(\text{mpba})_3]^{8-}$, is thus of the *meso*-helicite type and has a pseudo- C_{3h} symmetry. The entire octanuclear cluster, however, has a reduced C_1 symmetry because of the presence among the six peripheral metal atoms of both mer (Ni3, Ni4, Ni6, and Ni7) and fac (Ni5 and Ni8) isomers, with respect to the conformation of the dpt ligand. The peripheral nickel atoms adopt a distorted octahedral NiN_3O_3 geometry, with a $\text{Ni}-\text{O}(\text{water})$ average bond length (2.15 \AA) larger than the $\text{Ni}-\text{N}(\text{amine})$ and $\text{Ni}-\text{O}(\text{carbonyl})$ ones (2.09 \AA). The distance between the two central nickel atoms is $6.829(4) \text{ \AA}$, while those between central and peripheral ones are in the range $5.446(2)$ – $5.487(6) \text{ \AA}$.

The temperature dependence of the dc molar magnetic susceptibility (χ_M) of **2b** (Figure 2) is consistent with its

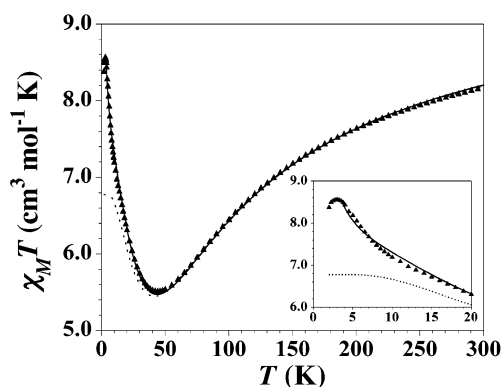


Figure 2. $\chi_M T$ versus T plot of **2b** under an applied field of 1 T ($T > 20$ K) and 250 G ($T < 20$ K). The inset shows the maximum of $\chi_M T$ in the low-temperature region. Solid and dotted lines are the best-fit curves for a $[\text{Ni}_4]_2$ molecule and two isolated Ni_4 molecules with $J_{\text{eff}} = 0$, respectively.

dimer-of-tetramers structure. The minimum of $\chi_M T$ around 45 K is characteristic of a moderately strong antiferromagnetic *intratetramer* coupling (J) between the central and the three peripheral Ni^{II} ions through the oxamate bridges. The propeller-type topology results in an incomplete spin cancellation and thus an $S = 2$ ground state for each tetranuclear unit. The maximum value of $\chi_M T$ at 3.0 K ($8.58 \text{ cm}^3 \text{ K mol}^{-1}$) is higher than expected for two isolated $S = 2$ Ni_4^{II} units ($\chi_M T = 6.9 \text{ cm}^3 \text{ K mol}^{-1}$, with $g = 2.15$). This suggests a weak ferromagnetic *intertetramer* coupling (J_{eff}) between the $S = 2$ ground states of the Ni_4^{II} units, yielding an $S = 4$ ground state for the entire octanuclear molecule. Yet, this maximum of $\chi_M T$ is lower than expected for an $S = 4$ Ni_8^{II} molecule ($\chi_M T = 11.3 \text{ cm}^3 \text{ K mol}^{-1}$, with $g = 2.15$). The slight decrease of $\chi_M T$ below 3.0 K (inset of Figure 2) is most likely due to zero-field splitting (ZFS) effects.

The magnetic susceptibility data of **2b** were fitted according to an effective spin Hamiltonian for a dimer-of-tetramers model that takes into account the coupling between the $S = 2$ ground state of each Ni_4^{II} unit [$H = -J(S_{1A}S_{3A} + S_{1A}S_{4A} + S_{1A}S_{5A} + S_{2B}S_{6B} + S_{2B}S_{7B} + S_{2B}S_{8B}) - J_{\text{eff}}S_A S_B + g\beta(S_{1A} + S_{3A} + S_{4A} + S_{5A} + S_{2B} + S_{6B} + S_{7B} + S_{8B})B$, with $S_{iA} = S_{jB} = 1$ for $i = 1, 3-5; j = 2, 6-8$; and $S_A = S_B = 2$].⁹ A least-squares fit gave $J = -26.6 \text{ cm}^{-1}$, $J_{\text{eff}} = +0.34 \text{ cm}^{-1}$, and $g = 2.13$. The theoretical curve closely follows the experimental data down to 5.0 K (solid line in Figure 2). The small $J_{\text{eff}}/|J|$ ratio confirms the validity of the perturbational treatment. The $-J$ value in **2b** is comparable to that reported for related oxalate-bridged (22.0 – 39.0 cm^{-1}) and oxamidate-bridged (25.0 – 57.0 cm^{-1}) binuclear nickel(II) complexes.^{10,11} In this model, the value of J_{eff} is related to that of J' between the two central Ni^{II} ions through the *meta*-phenylenediamidate bridges by $J_{\text{eff}} = 1/9 J'$,⁹ that is, $J' = +3.1$

(8) Crystal data for **2b**: $\text{C}_{66}\text{H}_{163}\text{Cl}_4\text{N}_{24}\text{Ni}_8\text{O}_{52.5}$, $M = 2744.4$, triclinic, space group $P1$, $a = 20.3117(3) \text{ \AA}$, $b = 17.8243(3) \text{ \AA}$, $c = 18.3675(3) \text{ \AA}$, $\alpha = 104.4870(10)^\circ$, $\beta = 115.9840(10)^\circ$, $\gamma = 92.9850(10)^\circ$, $V = 5686.82(16) \text{ \AA}^3$, $Z = 2$, $T = 293(2) \text{ K}$, $\mu(\text{Mo K}\alpha) = 1.487 \text{ mm}^{-1}$, 25 919 reflections measured, 19 048 assumed as observed with $I > 2\sigma(I)$. Refinement on F^2 of 1394 parameters with anisotropic thermal parameters for all non-hydrogen atoms gave $R = 0.0866$, $R_w = 0.2346$, and $\text{GOF} = 1.050$ (observed data).

(9) Aukauloo, A.; Ottenwaelder, X.; Ruiz, R.; Journaux, Y.; Pei, Y.; Riviere, E.; Muñoz, M. C. *Eur. J. Inorg. Chem.* **2000**, 951.

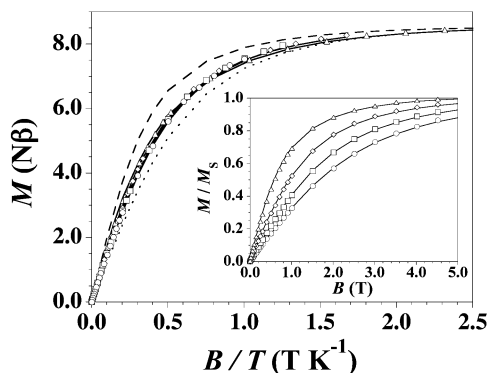


Figure 3. M versus B/T plot of **2b** at different temperatures: (Δ) 2.0, (\diamond) 3.0, (\square) 4.0, and (\circ) 5.0 K. Dashed and dotted lines are the Brillouin curves for an $S = 4$ state and two isolated $S = 2$ states, respectively, with $D = 0$. The inset shows the M/M_S versus B plot. Solid lines are the best-fit curves for a $[\text{Ni}_4]_2$ molecule with $D < 0$.

cm^{-1} .¹² The calculated J' value in **2b** agrees both in sign and in magnitude with that found in the binuclear precursor **1b** ($+3.6 \text{ cm}^{-1}$).¹³ This moderate ferromagnetic coupling is likely due to the spin polarization mechanism, as previously observed for related copper(II) complexes.^{7a,7c}

The field dependence of the dc magnetization (M) of **2b** in the temperature range 2.0–5.0 K (Figure 3) is consistent with a ferromagnetically coupled dimer of two $S = 2 \text{ Ni}^{\text{II}}_4$ units. At 2.0 K, the saturation magnetization value of 8.49 $N\beta$ is close to the expected one for an $S = 4$ state ($M_S = 8.6 \text{ N}$, with $g = 2.15$). Yet, the various isothermal curves are intermediate between the Brillouin functions of an $S = 4$ state and two isolated $S = 2$ states with $g = 2.15$ and no ZFS. This indicates the proximity of low-lying excited states of smaller spin values that are thermally populated. In the absence of ZFS, because of the relatively small J_{eff} value, four lowest excited spin states ($S = 3$, $S = 2$, $S = 1$, and $S = 0$) would be close in energy to the $S = 4$ ground state (at 1.4, 2.4, 3.1, and 3.4 cm^{-1} , respectively). On the other hand, the fact that the various isothermal curves in the M versus B/T plot do not perfectly superimpose at low B/T values suggests the presence of weak but nonnegligible ZFS of these low-lying $S = 4-1$ states.

Accordingly, the low-temperature magnetization data of **2b** were fitted by full-matrix diagonalization of an effective spin Hamiltonian for a dimer model that takes into account the axial magnetic anisotropy of the $S = 2$ ground state of each Ni^{II}_4 unit [$H = -J_{\text{eff}}S_{\text{A}}S_{\text{B}} + D_{\text{eff}}(S_{\text{zA}}^2 + S_{\text{zB}}^2) + g\beta(S_{\text{A}}$

$+ S_{\text{B}})B$, with $S_{\text{A}} = S_{\text{B}} = 2$].¹⁴ Least-squares fits with $J_{\text{eff}} = +0.34 \text{ cm}^{-1}$ fixed, gave $D_{\text{eff}} = +0.62 \text{ cm}^{-1}$ and $g = 2.16$ or, alternatively, $D_{\text{eff}} = -0.54 \text{ cm}^{-1}$ and $g = 2.15$. In both cases, the theoretical curves follow the experimental data fairly well (solid lines in the inset of Figure 3). The value of $|D_{\text{eff}}|$ is of the same magnitude as J_{eff} , which ensures a large mixing of the electronic spin states for **2b**. Hence, only the first two low-lying states are well separated from the others states, and according to the wave function composition, they are reminiscent of either the $M_S = 0, \pm 1$, levels of an $S = 4$ state if $D_{\text{eff}} > 0$, or the $M_S = \pm 4, \pm 3$, levels if $D_{\text{eff}} < 0$. The energy spectrum shows the $M_S = \pm 1$ excited state at 0.31 cm^{-1} from the $M_S = 0$ ground state if $D_{\text{eff}} > 0$, and it shows the $M_S = \pm 3$ excited state at 1.62 cm^{-1} from the $M_S = \pm 4$ ground state if $D_{\text{eff}} < 0$. The axial ZFS (D) of the $S = 4$ ground state can then be related to the energy difference (ΔE) between these two lowest levels by $\Delta E = D$ for $D_{\text{eff}} > 0$ or $\Delta E = -7D$ for $D_{\text{eff}} < 0$, that is, $D = +0.31$ or -0.23 cm^{-1} , respectively. The calculated $|D|$ value ultimately reflects both the single-ion magnetic anisotropy of high-spin Ni^{II} ions in a distorted octahedral coordination geometry and the structural anisotropy of the double-propeller $[\text{Ni}^{\text{II}}_4]_2$ cluster.¹⁵ Although the calculations do not allow resolution of the ambiguity in the sign of D for **2b**, a negative D value can be inferred from ac magnetic susceptibility measurements that revealed a frequency-dependent behavior typical of SMMs with $T_{\text{B}} \approx 3.0 \text{ K}$. Yet, the temperature dependence of the magnetic relaxation indicates a complex mechanism for the slow dynamics of the magnetization that is currently under investigation.¹⁶

In conclusion, the novel octanuclear nickel(II) coordination cluster **2b** is a high-spin and moderately anisotropic molecule built from the oxamate-based binuclear metallacryptand **1b** that acts as a ferromagnetic synthon. This rational complex-as-ligand approach shall lead to a variety of related homo- and heterometallic octanuclear complexes as potential SMMs.

Acknowledgment. This work was supported by the MCyT (Spain) (Projects BQU2001-2928 and BQU2001-3794) and the TMR Network “QuEMolNa” (European Union) (Contract MRTN-CT-2003-504880). E.P. and J.P. thank the MECyD (Spain) for grants.

Supporting Information Available: Preparation and characterization of **1b** and **2b**, dc magnetic susceptibility data of **1b**, ac magnetic susceptibility data of **2b**, and X-ray crystallographic data of **2b** in CIF format. This material is available free of charge via the Internet at <http://pubs.acs.org>.

IC048965X

- (10) Roman, P.; Guzman-Mirallas, C.; Luque, A.; Beitia, J. I.; Cano, J.; Lloret, F.; Julve, M.; Alvarez, S. *Inorg. Chem.* **1996**, *35*, 3741.
- (11) Lloret, F.; Sletten, J.; Ruiz, R.; Julve, M.; Faus, J.; Verdager, M. *Inorg. Chem.* **1992**, *31*, 778.
- (12) Least-squares fit of the magnetic susceptibility data of **2b** by full-matrix diagonalization of the appropriate spin Hamiltonian for an octamer model [$H = -J(S_1S_3 + S_1S_4 + S_1S_5 + S_2S_6 + S_2S_7 + S_2S_8) - J'S_1S_2 + g\beta(S_1 + S_2 + S_3 + S_4 + S_5 + S_6 + S_7 + S_8)B$] gave $J = -26.8 \text{ cm}^{-1}$, $J' = +3.2 \text{ cm}^{-1}$, and $g = 2.13$, in excellent agreement with the values obtained through the dimer-of-tetramers model.
- (13) Complex **1b** exhibits a magnetic behavior characteristic of a Ni^{II}_2 pair with weak ferromagnetic intrapair coupling (J) and appreciable axial ZFS (D) of the high-spin Ni^{II} ions (Figure S1, Supporting Information). A least-squares fit of the magnetic susceptibility data to the appropriate analytical expression derived from the spin Hamiltonian $H = JS_1S_2 + D(S_{1z}^2 + S_{2z}^2) + g\beta(S_1 + S_2)B$ (with $S_1 = S_2 = 1$) gave $J = +3.6 \text{ cm}^{-1}$, $D = 3.5 \text{ cm}^{-1}$, and $g = 2.14$.

- (14) Wernsdorfer, W.; Aliaga-Alcalde, N.; Hendrickson, D. N.; Christou, G. *Nature* **2002**, *416*, 406.
- (15) Cornia, A.; Fabretti, A. C.; Garrisi, P.; Mortal, C.; Bonacchi, D.; Gatteschi, D.; Sessoli, R.; Sorace, L.; Wernsdorfer, W.; Barra, A. L. *Angew. Chem., Int. Ed.* **2004**, *43*, 1136.
- (16) The relaxation time (τ) of **2b** follows the Arrhenius law characteristic of a thermally activated mechanism, $\tau = \tau_0 \exp(U/k_{\text{B}}T)$, with $\tau_0 = 1.2 \times 10^{-16} \text{ s}$ and $U = 71.3 \text{ cm}^{-1}$ (Figure S2, Supporting Information). Yet, the calculated preexponential factor (τ_0) is abnormally low compared to those of other SMMs. Moreover, assuming that the slow relaxation stems exclusively from the $S = 4$ ground state, the D value of -4.5 cm^{-1} estimated through the expression $U = |D|S^2$ is far above that derived from dc magnetization data.